

REPELLING DYNAMICS NEAR A BYKOV CYCLE

ALEXANDRE A. P. RODRIGUES

ABSTRACT. What set does an experimenter see while simulating numerically the dynamics of a Bykov cycle? In this paper, we discuss the fate of typical trajectories near a Bykov cycle for a C^1 -vector field and we establish that despite the existence of shift dynamics (chaos) nearby, Lebesgue-almost all trajectories starting in a small neighbourhood of a Bykov cycle are repelled.

1. INTRODUCTION

In the context of diffeomorphisms, dynamic complexity and the presence of homoclinic orbits are closely related. This relationship has been discovered by Henri Poincaré [24] more than 120 years ago, in the framework of the *Three Body Problem*. Almost 50 years later, David Birkhoff [4, 5] proved that near a transversal homoclinic cycle, there exists a complex and an intricated set of periodic solutions, with a very large period. In the sixties, Steven Smale [32] constructed a geometrical scheme in a neighbourhood of a transversal homoclinic point – the *Smale horseshoe*, which explained the Birkhoff results. The Smale horseshoe organized the dynamics that occur near a homoclinic cycle through a conjugation to Bernoulli's shifts.

Also in the sixties, in the context of vector fields, L. P. Shilnikov [29, 30, 31] demonstrated that in a neighbourhood of an unstable homoclinic cycle associated to a saddle-focus, there exists a countable set of periodic trajectories following the cycle. In fact, this result is related to that of Birkhoff for diffeomorphisms: the non-trivial closed trajectories that appear near the cycle are the result of a suspension of infinitely many horseshoes. Nowadays, a particularly important subject in the theory of nonlinear dynamical systems is the study of the behaviour near homoclinic and heteroclinic cycles associated to all kind of invariant saddles. These structures have been invoked to explain several dynamic phenomena in which a system repeatedly seems to switch between different dynamical states.

In three dimensional flows, the unstable homoclinic cycle associated to a saddle-focus provides one of the main examples for the occurrence of chaos, involving hyperbolic horseshoes. When the vector field is perturbed in order to break the homoclinic cycle, such horseshoes are destroyed and it may appear persistent strange attractors as those described in Mora and Viana [21]. Under additional assumptions, infinitely many strange attractors may coexist in a persistent way – see Homburg [13].

After the classical Shilnikov homoclinic cycles associated to a single saddle-focus, *Bykov cycles* are the simplest heteroclinic cycles between two saddle-foci where one heteroclinic connection is structurally stable and the other is not. These cycles, also called by *T-points*, are codimension two bifurcation heteroclinic cycles that involve two saddle-foci of different Morse indices. They have been first studied by Bykov [9] and recently there has been a renewal of interest of this type of heteroclinic bifurcation in different situations – see Sánchez *et al* [10], Ibáñez and Rodríguez [15] and Labouriau and Rodrigues [26]. In this paper, we are interested in the “size” of the *basin of attraction* of a Bykov cycle, which has not always attracted appropriate attention.

There are different concepts of what we may call an *attracting set* for a dynamical system, such as the maximal attractor, the non-wandering set, the Milnor's attractor or the statistical attractor; the notion of attractor is important for understanding the long-term behaviour of trajectories of the system – see Buesco [8] and Milnor [20].

2000 *Mathematics Subject Classification*. Primary: 37C29; Secondary: 34C28, 37C27, 37C20.

Key words and phrases. Bykov cycle, repelling dynamics, Generalized Conley-Morse conditions, C^1 -vector fields.

CMUP is supported by the European Regional Development Fund through the programme COMPETE and by the Portuguese Government through the Fundação para a Ciência e a Tecnologia (FCT) under the project PEst-C/MAT/UI0144/2011. A.A.P. Rodrigues was supported by the grant SFRH/BD/28936/2006 of FCT.

In order to explain these notions of attraction, other concepts of stability for heteroclinic cycles sets were introduced in the literature – they do not require attraction in a full open set; they may even be repelling in a cusped region in cross sections transverse to the heteroclinic network – see for instance Brannath [3] or the article of Podvigina and Aswhin [23]. They define a heteroclinic cycle to be *essentially asymptotically stable* if it attracts Lebesgue–almost all nearby trajectories; similarly we may define it to be *almost completely unstable* if the network repels Lebesgue–almost all trajectories.

Symmetry is a natural setting for persistent heteroclinic cycles. In this context, Krupa and Melbourne [17, 18] gave a sufficient condition (also necessary when some additional conditions are satisfied) for a heteroclinic cycle to be *asymptotically stable*: trajectories near the heteroclinic cycle will follow and approach it when $t \rightarrow +\infty$; it attracts all nearby points.

In [1, 19], the authors constructed an explicit ordinary differential equation in the unit sphere \mathbf{S}^3 that is $(\mathbf{SO}(2) \oplus \mathbf{Z}_2)$ – equivariant whose flow contains an asymptotically stable heteroclinic network involving two saddle-foci with different Morse indices. Breaking the rotational symmetry, the authors proved analytically the transverse intersection of the invariant two-dimensional manifolds of the equilibria and thus the existence of a *Bykov cycle* in its unfolding. Another codimension three bifurcation possessing cycles of this type has been studied by [25], in the context of the geodynamo problem. In Labouriau and Rodrigues [26], it is given a description of the geometry of a nested sequence of suspended horseshoes that exists in a neighbourhood of the Bykov cycle. It is a well known result that a hyperbolic invariant set of a C^2 -diffeomorphism has zero Lebesgue measure – see Bowen [7]. However, since the authors of [26] worked in the C^1 -category, this chain of horseshoes may have positive Lebesgue measure as the “Bowen horseshoe” described in [6].

In this paper, we show that though the existence of a sequence of suspended horseshoes accumulating on the Bykov cycle, it just involves a portion with zero Lebesgue measure of a tubular neighbourhood of the cycle. This means that the Cantor set found in [26] is not “fat” as the transitive set constructed by Bowen [6]. To tackle the problem, we construct a cross section Σ near a Bykov cycle and we prove that the set of initial conditions that return to Σ for all time, has zero Lebesgue measure. In our plan, we use the *Generalized Conley and Moser conditions* – Moser [22] (recent approach in Koon *et al* [16] and Wiggins [34]): they are verifiable conditions for the first return map to Σ , to possess an invariant set Λ on which it is topologically conjugate to a shift acting on bi-infinite sequences constructed from a countable set of symbols. With this technique, we are able to prove that the chaos does not trap most trajectories in the neighbourhood of the cycle – almost all solutions leave any neighbourhood of the Bykov cycle. This argument explains the title.

2. PRELIMINARIES

Let f be a C^1 vector field on \mathbf{R}^n with flow given by the unique solution $x(t) = \varphi(t, x_0) \in \mathbf{R}^n$ of $\dot{x} = f(x)$ and $x(0) = x_0$. Given two equilibria p and q , an m -dimensional *heteroclinic connection* from p to q , denoted $[p \rightarrow q]$, is an m -dimensional connected flow-invariant manifold contained in $W^u(p) \cap W^s(q)$. There may be more than one connection from p to q .

Let $\mathcal{S} = \{p_j : j \in \{1, \dots, k\}\}$ be a finite ordered set of mutually disjoint invariant saddles. Following Field [11], we say that there is a *heteroclinic cycle* associated to \mathcal{S} if

$$\forall j \in \{1, \dots, k\}, W^u(p_j) \cap W^s(p_{j+1}) \neq \emptyset \pmod{k}.$$

Sometimes, we refer to the equilibria defining the heteroclinic cycle as *nodes*. A *heteroclinic network* is a finite connected union of heteroclinic cycles. All nodes are hyperbolic; the dimension of the local unstable manifold of an equilibria p will be called the *Morse index* of p .

In a three-dimensional manifold, a *Bykov cycle* is a heteroclinic cycle associated to two hyperbolic saddle-foci with different Morse indices, in which the one-dimensional manifolds coincide and the two-dimensional invariant manifolds have a transverse intersection – see figure 1. A Bykov cycle is also called by *T-point* because it corresponds to a point on the space of parameters where such cycles appear. The existence of such cycles implies the existence of a bigger network, which we call hereafter a *Bykov network* – details in Labouriau and Rodrigues [26] (proposition 2, item 4): beyond the original transverse connections, there exists infinitely many subsidiary heteroclinic connections turning around the original Bykov cycle.

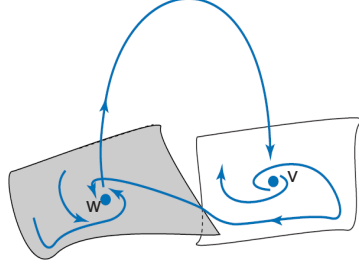


FIGURE 1. *Bykov cycle in a three-dimensional manifold*: heteroclinic cycle associated to two hyperbolic saddle-foci with different Morse indices, in which the one-dimensional manifolds coincide and the two-dimensional invariant manifolds have a transverse intersection. They are robust in vector fields that commute with involutions.

Let $x_0 \in W^u(p_j) \cap W^s(p_{j+1})$. Denoting by $T_{x_0}W^u(p_j)$ and $T_{x_0}W^s(p_{j+1})$ the tangent spaces to $W^u(p_j)$ and $W^s(p_{j+1})$ at x_0 , respectively, we say that the manifolds $W^u(p_j)$ and $W^s(p_{j+1})$ intersect transversely at x_0 if:

$$(1) \quad \dim T_{x_0}W^u(p_j) + \dim T_{x_0}W^s(p_{j+1}) - n = \dim [T_{x_0}W^u(p_j) \cap T_{x_0}W^s(p_{j+1})].$$

Recall that if two surfaces intersect transversely at some point, thus any two C^1 -close surfaces intersect transversely at a nearby point. Although the concept of transversality is stated at x_0 , condition (1) is independent of the choice of the point x_0 in the heteroclinic connection.

We recall the definition of a Milnor attractor – for more details we refer the reader to Milnor [20]. Let ℓ denote a measure on a smooth manifold M locally equivalent to the Lebesgue measure on charts (ℓ can be the measure defined by the Riemannian volume form). If Z is a measurable subset of M with $\ell(M) \neq 0$, we let $\mathcal{F}(Z)$ denote the set of measurable subsets Z' of Z such that $\ell(Z \setminus Z') = 0$. Given $x \in M$, let $\omega(x) = \bigcap_{T>0} \{\varphi(t, x) : t \geq T\}$ denote the ω -limit set of the solution through x . If $X \subset M$ is a compact and flow-invariant subset, we let $\mathcal{B}(X) = \{x \in M : \omega(x) \subset X\}$ denote the *basin of attraction* of X . A compact invariant subset X of M is a *Milnor attractor* if $\ell(\mathcal{B}(X)) > 0$ and for any proper compact invariant subset Y of X , $\ell(\mathcal{B}(X) \setminus \mathcal{B}(Y)) > 0$.

3. MAIN RESULT AND FRAMEWORK OF THE PAPER

Our object of study is the dynamics around a *Bykov cycle*, for which we give a rigorous description here. The cycle lies in a topological three-sphere and in which the nodes are saddle-foci. Specifically, we study a C^1 -vector field f on \mathbf{S}^3 whose flow has the following properties (see figure 1):

- (H1) There is a heteroclinic network Γ associated to two hyperbolic saddle-foci of different Morse index \mathbf{v} and \mathbf{w} (the Morse indices of \mathbf{v} and \mathbf{w} are 1 and 2, respectively). The eigenvalues of df_X are
 - (a) $-C_{\mathbf{v}} \pm i$ and $E_{\mathbf{v}}$ with $C_{\mathbf{v}} \neq E_{\mathbf{v}} > 0$, for $X = \mathbf{v}$;
 - (b) $E_{\mathbf{w}} \pm i$ and $-C_{\mathbf{w}}$ with $C_{\mathbf{w}} \neq E_{\mathbf{w}} > 0$, for $X = \mathbf{w}$.
- (H2) There is a one-dimensional heteroclinic connection from \mathbf{v} to \mathbf{w} .
- (H3) There is at least one heteroclinic connection from \mathbf{w} to \mathbf{v} and the two-dimensional manifolds meet transversely at these connections.
- (H4) There are open neighbourhoods V and W of \mathbf{v} and \mathbf{w} , respectively, such that for any trajectory going from V to W , the direction of its turning around $[\mathbf{v} \rightarrow \mathbf{w}]$ is the same in V and in W (see figures 2 and 3).

Hypothesis (H4) may have a more formal formulation. Let V and W be small neighbourhoods of \mathbf{v} and \mathbf{w} , respectively. Consider a solution $\varphi(t)$ that starts at the boundary of V , ∂V , goes inside V where it turns infinitely many times around the heteroclinic connection $[\mathbf{v} \rightarrow \mathbf{w}]$, then leaves the neighbourhood V , goes into W where it makes several turns again before arriving at the boundary of W , ∂W . If (H4) holds, then for all trajectories φ as above, the *concatenation property* is valid:

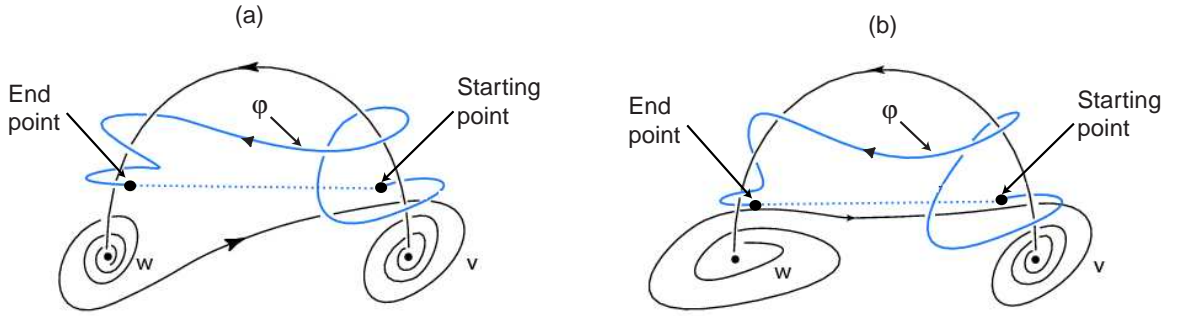


FIGURE 2. There are two different possibilities for the geometry of the flow around Γ depending on the direction trajectories turn around the heteroclinic connection $[\mathbf{v} \rightarrow \mathbf{w}]$. (a): The direction of turning around $[\mathbf{v} \rightarrow \mathbf{w}]$ is the same in V and W ; (b): The direction of turning around $[\mathbf{v} \rightarrow \mathbf{w}]$ in V is the opposite of that in W . Courtesy: Isabel S. Labouriau.

(H4^{*}) if one joins the starting point of φ in ∂V and in ∂W , one obtains a closed curve that is linked to the heteroclinic cycle Γ (case (a) of figure 2).

Condition (H4^{*}) means that the curve φ and the cycle cannot be separated by any isotopy. Now we state the main result which guarantees the repelling scenario near the cycle: Lebesgue–almost all solutions starting nearby the Bykov cycle Γ go away.

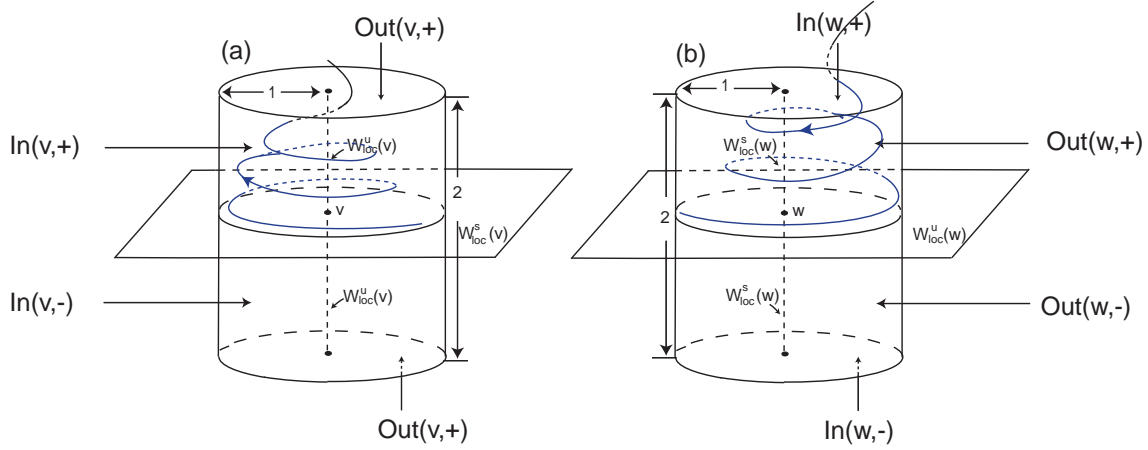
Theorem 1. *Let \mathcal{V} be a small neighbourhood of Γ . If Γ satisfies conditions (H1) – (H4), then there exists a cross section Σ transverse to Γ such that the set of initial conditions in $\Sigma \cap \mathcal{V}$ that do not leave \mathcal{V} for all time, has zero Lebesgue measure.*

Theorem 1 shows that the nested sequence of horseshoes whose existence is proved in [26] occupies a zero Lebesgue measure; thus the shift dynamics does not trap most trajectories in the neighbourhood of the Bykov cycle. In particular, the cycle cannot be a Milnor attractor. With this result, we may conclude that the heteroclinic infinite switching ensured in Aguiar *et al* [2] and Labouriau and Rodrigues [26] is realized by a set of initial conditions with zero Lebesgue measure.

The rest of this paper is organized as follows: in section 4, applying C^1 –coordinate changes, we linearize the vector field f around the saddle-foci; we introduce some notation that will be used in the rest of the article and we obtain a geometrical description of the way the flow transforms a curve of initial conditions lying across the stable manifold of an equilibrium. In section 5, we explore this geometrical setting to construct a set of horizontal and vertical rectangles on which the Generalized Conley-Moser conditions may be applied. We prove that the set of points that return to a section transverse to the Bykov cycle Γ has zero Lebesgue measure. The proof in section 5 is subject to the restriction on the connection map from \mathbf{v} to \mathbf{w} , which we assume to be the identity. In section 6, we remove this assumption and we show how our methods easily extend to a general transition map. We end this article with a short discussion of the results. Throughout this paper, we have endeavoured to make a self contained exposition bringing together all topics related to the proofs. We have stated short lemmas and we draw illustrative figures to make the paper easily readable.

4. CONSTRUCTION OF THE POINCARÉ MAPS

In this section, we establish local coordinates near the saddle-foci \mathbf{v} and \mathbf{w} and we define some terminology that will be used in the rest of the paper. The crucial point is the application of Samovol’s Theorem to C^1 –linearize the flow around the equilibria and to introduce cylindrical coordinates around each node – see also Homburg and Sandstede [14] (section 3.1). We use neighbourhoods with boundary transverse to the linearized flow.


 FIGURE 3. Cylindrical neighbourhoods of the saddle-foci \mathbf{v} (a) and \mathbf{w} (b).

4.1. Construction of the local maps. By (H1), since $C_{\mathbf{v}} \neq E_{\mathbf{v}}$ and $C_{\mathbf{w}} \neq E_{\mathbf{w}}$, by Samovol's Theorem [28], the vector field f is C^1 -conjugated to its linear part around each saddle-focus. In cylindrical coordinates (ρ, θ, z) the linearizations at X are given by:

$$(2) \quad X = \mathbf{v} : \quad \dot{\rho} = -C_{\mathbf{v}}\rho \quad \wedge \quad \dot{\theta} = 1 \quad \wedge \quad \dot{z} = E_{\mathbf{v}}z$$

$$(3) \quad X = \mathbf{w} : \quad \dot{\rho} = E_{\mathbf{w}}\rho \quad \wedge \quad \dot{\theta} = 1 \quad \wedge \quad \dot{z} = -C_{\mathbf{w}}z.$$

After a linear rescaling of the local variables, we consider cylindrical neighbourhoods of \mathbf{v} and \mathbf{w} in \mathbf{S}^3 of radius 1 and height 2 that we denote by V and W , respectively – see figure 3. Their boundaries consist of three components: the cylinder wall parametrized by $x \in \mathbf{R} \pmod{2\pi}$ and $|y| \leq 1$ with the usual cover $(x, y) \mapsto (1, x, y) = (\rho, \theta, z)$ and two disks (top and bottom of V). We take polar coverings of these disks $(r, \varphi) \mapsto (r, \varphi, j) = (\rho, \theta, z)$ where $j \in \{-1, +1\}$, $0 \leq r \leq 1$ and $\varphi \in \mathbf{R} \pmod{2\pi}$.

The cylinder wall is denoted by $In(\mathbf{v})$. Later, it will be useful the distinction of the two connected components of $In(\mathbf{v})$: the set of points in $In(\mathbf{v})$ with positive (resp. negative) second coordinate is denoted by $In(\mathbf{v}, +)$ (resp. $In(\mathbf{v}, -)$), as shown in figure 3 (a). The top and the bottom of the cylinder are denoted, respectively, by $Out(\mathbf{v}, +)$ and $Out(\mathbf{v}, -)$. Note that $W_{loc}^s(\mathbf{v})$ corresponds to the circle $y = 0$. The boundary of V can be written as the disjoint union

$$\partial V = In(\mathbf{v}) \dot{\cup} Out(\mathbf{v}) \dot{\cup} \Omega_{\mathbf{v}},$$

where $\Omega_{\mathbf{v}}$ is the part of ∂V where the flow is not transverse. It follows by the above construction that:

Lemma 2. For each $j \in \{+, -\}$, solutions starting at:

- (1) interior points of $In(\mathbf{v}, j)$ go inside the cylinder V in positive time;
- (2) interior points of $Out(\mathbf{v}, j)$ go inside the cylinder V in negative time;
- (3) $In(\mathbf{v}) \setminus W^s(\mathbf{v})$, leave V at $Out(\mathbf{v}, j)$.

For each node, we obtain the expression of the local map that sends points in the boundary where the flow goes in, into points in the boundary where the flows goes out. The local map $\Phi_{\mathbf{v}} : In(\mathbf{v}, +) \rightarrow Out(\mathbf{v}, +)$ near \mathbf{v} is given by

$$(4) \quad \Phi_{\mathbf{v}}(x, y) = \left(y^{\delta_{\mathbf{v}}}, -\frac{\ln y}{E_{\mathbf{v}}} + x \right) = (r, \phi)$$

where $\delta_{\mathbf{v}} = \frac{C_{\mathbf{v}}}{E_{\mathbf{v}}} \neq 1$ is the saddle index of \mathbf{v} . For $y < 0$, the expression for the local map from $In(\mathbf{v}, -)$ to $Out(\mathbf{w}, -)$ is given by $\Phi_{\mathbf{v}}(x, -y)$.

Similarly, after linearization and rescaling of the local variables, we get dual cross sections near \mathbf{w} . We omit the details because they are similar to those of \mathbf{v} . The set $W_{loc}^s(\mathbf{w})$ is the z -axis, intersecting the top and bottom of the cylinder W at the origin of its coordinates – see figure 3 (b). The set $W_{loc}^u(\mathbf{w})$ is parametrized by $z = 0$. We denote by $In(\mathbf{w}, j)$, $j \in \{-, +\}$, the two components of $In(\mathbf{w})$, top and bottom. By construction, we may easily conclude that:

Lemma 3. *For each $j \in \{+, -\}$, solutions starting at:*

- (1) *interior points of $In(\mathbf{w}, j)$ go into W in positive time;*
- (2) *interior points of the cylinder wall $Out(\mathbf{w}, j)$ go into W in negative time;*
- (3) *at $In(\mathbf{w}, j) \setminus W^s(\mathbf{w})$, leave the cylindrical neighbourhood at $Out(\mathbf{w}, j)$.*

The local map $\Phi_{\mathbf{w}} : In(\mathbf{w}, +) \setminus W_{loc}^s(\mathbf{w}) \rightarrow Out(\mathbf{w}, +)$ near \mathbf{w} is given by:

$$(5) \quad \Phi_{\mathbf{w}}(r, \varphi) = \left(-\frac{\ln r}{E_{\mathbf{w}}} + \varphi, r^{\delta_{\mathbf{w}}} \right) = (x, y) ,$$

where $\delta_{\mathbf{w}} = \frac{C_{\mathbf{w}}}{E_{\mathbf{w}}} \neq 1$ is the saddle index of \mathbf{w} . The same expression holds for the local map from $In(\mathbf{w}, -) \setminus W_{loc}^s(\mathbf{w})$ to $Out(\mathbf{w}, -)$, with the exception that the second coordinate of $\Phi_{\mathbf{w}}$ changes its sign.

4.2. Local geometry. Now, we will use the maps (4) and (5) to study the geometry associated to the dynamics around each saddle-focus. We start with some definitions, which generalize the concepts introduced in Rodrigues *et al* [27].

- (1) A *segment β on $In(\mathbf{v})$* is a smooth regular parametrized curve of the type

$$\beta : [0, 1) \rightarrow In(\mathbf{v})$$

that meets $W_{loc}^s(\mathbf{v})$ transversely at the point $\beta(1)$ only and such that, writing $\beta(s) = (x(s), y(s))$, both x and y are monotonic functions of s – see figure 4 (a).

- (2) A *generalized spiral on $Out(\mathbf{v})$ or $In(\mathbf{w})$ around a point p* is a curve

$$\alpha : [0, 1) \rightarrow Out(\mathbf{v}) \quad \text{or} \quad \alpha : [0, 1) \rightarrow In(\mathbf{w})$$

satisfying $\lim_{s \rightarrow 1^-} \alpha(s) = p$ and such that, if $\alpha(s) = (r(s), \theta(s))$ are its expressions in polar coordinates around p , then $\lim_{s \rightarrow 1^-} |\theta(s)| = +\infty$: see figure 4 (a) and (b). If the maps r and θ are monotonic, we say that α is a *spiral*.

- (3) Let $a, b \in \mathbf{R}$ such that $a < b$ and let $Out(\mathbf{w})$ be a surface parametrized by a covering $(\theta, h) \in \mathbf{R} \times [a, b]$ where θ is periodic. A *generalized helix on $Out(\mathbf{w})$ accumulating on the circle $h = h_0$* is a curve

$$\gamma : [0, 1) \rightarrow Out(\mathbf{w})$$

such that its coordinates $(\theta(s), h(s))$ satisfy $\lim_{s \rightarrow 1^-} h(s) = h_0$ and $\lim_{s \rightarrow 1^-} |\theta(s)| = +\infty$ – see figure 4 (b). If the maps θ and h are monotonic, we say that γ is a *helix*.

The next proposition summarizes some basic technical results about the geometry near each saddle-focus. The proof may be found in section 6 of Aguiar *et al* [2] – this is why it will be omitted here.

Proposition 4. *For $j \in \{+, -\}$:*

- (1) *a segment β on $In(\mathbf{v}, j)$ is mapped by $\Phi_{\mathbf{v}}$ into a spiral on $Out(\mathbf{v}, j)$ around $W_{loc}^u(\mathbf{v})$;*
- (2) *if (H4) holds, a spiral on $In(\mathbf{w}, j)$ around $W_{loc}^s(\mathbf{w})$ is mapped by $\Phi_{\mathbf{w}}$ into a helix on $Out(\mathbf{w}, j)$ accumulating on the circle $Out(\mathbf{w}, j) \cap W^u(\mathbf{w})$.*

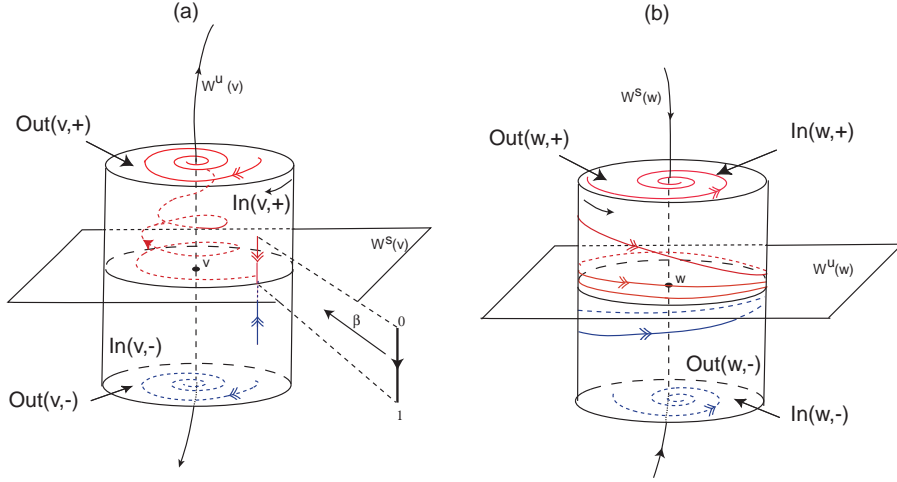


FIGURE 4. (a): A segment β on $In(\mathbf{v})$ is mapped by $\Phi_{\mathbf{v}}$ into a spiral on $Out(\mathbf{v})$ around $W_{loc}^u(\mathbf{v})$; (b): A spiral α on $In(\mathbf{w})$ is mapped by $\Phi_{\mathbf{w}}$ into a helix on $Out(\mathbf{w})$ accumulating on $W_{loc}^u(\mathbf{w})$. Note that the arrows on the segment, spirals and helices indicate correspondence of orientation and not the flow.

4.3. Transition Maps. From now on, we establish a convention for the transition maps from the neighbourhood V to W . In the rest of this paper, we study the Poincaré first return map on the boundaries defined in these sections. Consider the transition maps where $j = +, -$:

$$\Psi_{\mathbf{v} \rightarrow \mathbf{w}} : Out(\mathbf{v}, j) \longrightarrow In(\mathbf{w}, j) \quad \text{and} \quad \Psi_{\mathbf{w} \rightarrow \mathbf{v}} : Out(\mathbf{w}, j) \longrightarrow In(\mathbf{v}, j).$$

The linear part of the map $\Psi_{\mathbf{v} \rightarrow \mathbf{w}}$ may be represented, in rectangular coordinates (X, Y) , as the composition of a rotation of the coordinate axes and a change of scales. As in Bykov [9] and Homburg and Sandstede [14], after a rotation and a uniform rescaling of the coordinates, we may assume without loss of generality that $\Psi_{\mathbf{v} \rightarrow \mathbf{w}}$ is given by the linear map:

$$(6) \quad \begin{pmatrix} a & 0 \\ 0 & \frac{1}{a} \end{pmatrix} + \dots \quad a \in \mathbf{R}^+,$$

where the dots mean smooth functions which tend to zero as $X, Y \rightarrow 0$. Note that the map $\Psi_{\mathbf{v} \rightarrow \mathbf{w}}$ is given in rectangular coordinates (X, Y) . To compose this map with $\Phi_{\mathbf{v}}$ or $\Phi_{\mathbf{w}}$, it is required to change the coordinates, which may be intractable.

By (H3), the manifolds $W^u(\mathbf{w})$ and $W^s(\mathbf{v})$ intersect transversely. Thus the map $\Psi_{\mathbf{w} \rightarrow \mathbf{v}}$ can be seen as a rotation by an angle $\alpha \neq 0$. Without loss of generality, we use $\alpha \equiv \frac{\pi}{2}$, that simplifies the computations and the expressions used.

In section 5, we will assume that the map $\Psi_{\mathbf{v} \rightarrow \mathbf{w}}$ is the identity ($a = 1$); nevertheless all the results follow straightforwardly if $\Psi_{\mathbf{v} \rightarrow \mathbf{w}}$ is a uniform contraction or a uniform expansion defined respectively by the matrices ($a > 1$):

$$\begin{pmatrix} a & 0 \\ 0 & a \end{pmatrix} \quad \text{and} \quad \begin{pmatrix} \frac{1}{a} & 0 \\ 0 & \frac{1}{a} \end{pmatrix}.$$

In section 6, we remove the assumption that $a = 1$. In other terms, we assume that $\Psi_{\mathbf{v} \rightarrow \mathbf{w}}$ takes the general form (6) – and we conclude that theorem 1 is still valid. In the sequel, we will make use of the subscripts $(1, 1)$, (a, a) , $(\frac{1}{a}, \frac{1}{a})$ or $(a, \frac{1}{a})$, which mean that the transition map (in rectangular coordinates) from \mathbf{v} to \mathbf{w} is the identity, a uniform expansion, a uniform contraction or the general form (6), respectively. When it is clear, we omit the subscripts.

5. REPELLING DYNAMICS

Let \mathcal{V} be a small topological neighbourhood of the heteroclinic network Γ containing V and W , neighbourhoods of \mathbf{v} and \mathbf{w} , in which Samovol's theorem holds. Let $P_{\mathbf{w}}$ and $P_{\mathbf{v}}$ be the points where

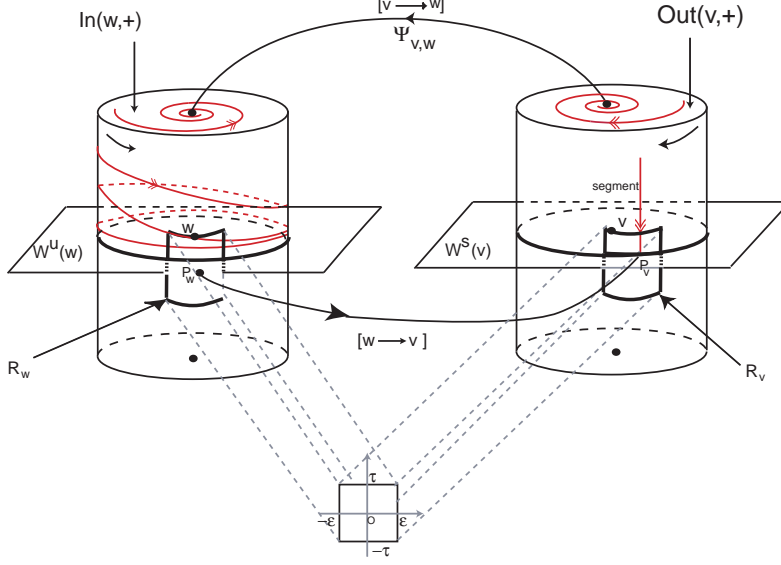


FIGURE 5. Local parametrization of R_v and R_w and transition from \mathbf{v} to \mathbf{w} . A segment in $In(\mathbf{v})$ is mapped into a spiral on $Out(\mathbf{v})$ around $W_{loc}^u(\mathbf{v}) \cap Out(\mathbf{v})$. By flow box fashion, this spiral is mapped into another spiral on $In(\mathbf{w})$ around $W_{loc}^s(\mathbf{w}) \cap In(\mathbf{w})$, which is mapped into a helix on $Out(\mathbf{w})$ accumulating on $W_{loc}^u(\mathbf{w})$ and crossing infinitely many times R_w .

$[\mathbf{w} \rightarrow \mathbf{v}]$ meets $Out(\mathbf{w})$ and $In(\mathbf{v})$, respectively as shown in figure 5. Of course $P_w \in W_{loc}^u(\mathbf{w})$ and $P_v \in W_{loc}^s(\mathbf{v})$. Without loss of generality, assume that in local coordinates, the angular component of these two points is $0 \pmod{2\pi}$.

For small $\varepsilon > 0$ and $\tau \in (0, 1]$, the rectangle $[-\varepsilon, \varepsilon] \times [-\tau, \tau]$ is mapped into $Out(\mathbf{w})$ and $In(\mathbf{v})$ by the local parametrizations of $Out(\mathbf{w})$ and $In(\mathbf{v})$. Hereafter, their images will be denoted, respectively, by R_w and R_v – they correspond to *rectangles on $Out(\mathbf{w})$ and $In(\mathbf{v})$ centered at P_w and P_v , respectively* – see figure 5.

As we have said at the end of section 4, here we assume that the map $\Psi_{\mathbf{v} \rightarrow \mathbf{w}}$ is the identity; all computations hold if $\Psi_{\mathbf{v} \rightarrow \mathbf{w}}$ is a uniform contraction or an expansion. We denote the map $\Phi_w \circ \Psi_{\mathbf{v} \rightarrow \mathbf{w}} \circ \Phi_v$ by $\eta_{(1,1)}$ or simply by η . Let $R_{(1,1)}$ be the first return map to R_v : $R_{(1,1)} \equiv \Psi_{\mathbf{w} \rightarrow \mathbf{v}} \circ \eta_{(1,1)}$.

Proposition 5. *Let $\gamma(x_0)$ be a vertical segment on R_v whose angular component is $x_0 \in \mathbf{R} \pmod{2\pi}$. Then there are $n_0 \in \mathbf{N}$ and a family of intervals $(\mathcal{I}_n)_{n \geq n_0} = ([a_n, b_n])_{n \geq n_0}$, where:*

$$a_n = K^{-1}(-\varepsilon - 2n\pi + x_0), \quad b_n = K^{-1}(\varepsilon - 2n\pi + x_0) \quad \text{and} \quad K = \frac{C_v + E_w}{E_v E_w} > 0,$$

such that each interval $[a_n, b_n] \subset \text{graph}(\gamma)$ and satisfies $\eta_{(1,1)}([e^{a_n}, e^{b_n}]) \subset R_w$ (see figure 7).

Note that a_n and b_n depend continuously on $x \in [-\varepsilon, \varepsilon]$. In the following proof, we omit the subscript $(1, 1)$.

Proof. Write $\gamma(s) = (x_0, y^*(s)) \in R_v \subset In(\mathbf{v}, +)$, where $y^*(s) \geq 0$ is a decreasing map and $\lim_{s \rightarrow 1^-} \gamma(s) = 0$. The function Φ_v maps the curve γ into a spiral parametrized by:

$$\Phi_v(\gamma(s)) = \Phi_v[(x_0, y^*(s))] = \left[y^*(s)^{\delta_v}, -\frac{\ln(y^*(s))}{E_v} + x_0 \right] = (r(s), \phi(s)).$$

The map $\Phi_v \circ \gamma$ is a spiral because $r(s)$ and $\phi(s)$ are monotonic (since y is monotonic) and

$$\lim_{s \rightarrow 1^-} y^*(s)^{\delta_v} = 0 \quad \text{and} \quad \lim_{s \rightarrow 1^-} -\frac{\ln(y^*(s))}{E_v} + x_0 = +\infty.$$

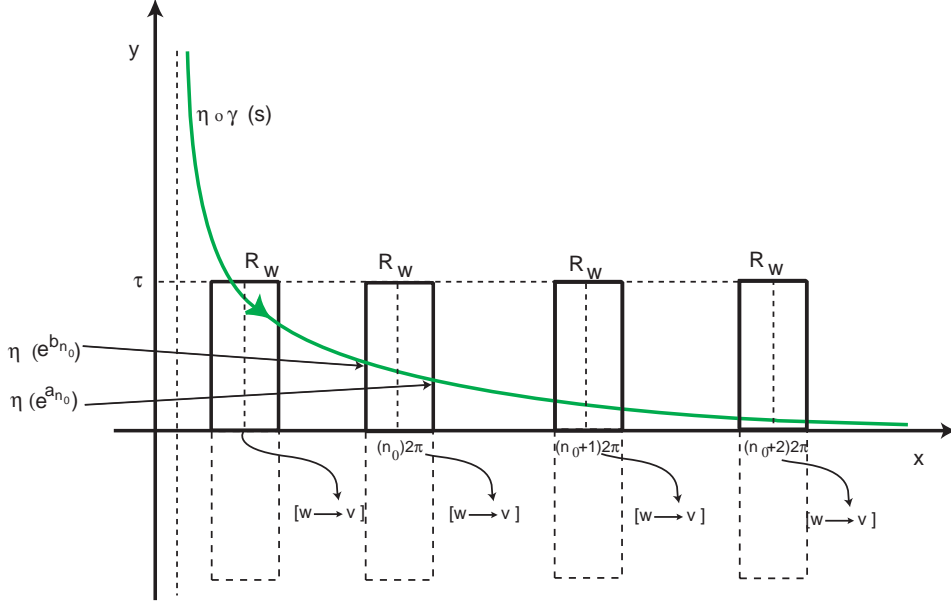


FIGURE 6. A helix on a periodic cover of $Out(\mathbf{w})$. Once the helix meets the first rectangle, it will intersect the rectangle infinitely many times at intervals whose images accumulate on $W_{loc}^u(\mathbf{w})$ represented by $y = 0$.

The analytical expression of $\eta \circ \gamma$ is given by:

$$\eta \circ \gamma(s) = (-K \ln(y^*(s)) + x_0; y^*(s)^\delta) = (x(s), y(s))$$

where

$$K = \frac{C_{\mathbf{v}} + E_{\mathbf{w}}}{E_{\mathbf{v}} E_{\mathbf{w}}} > 0 \quad \text{and} \quad \delta = \delta_{\mathbf{v}} \delta_{\mathbf{w}} \neq 0.$$

The coordinates (x, y) in $Out(\mathbf{w})$ are chosen so as to make the angular coordinate x an increasing or decreasing function of s in a consistent way – note that we are using the hypothesis (H4): the direction of turning of any trajectory around $[\mathbf{v} \rightarrow \mathbf{w}]$, when it is going from V to W , is the same in V and in W . The resulting curve, $\eta \circ \gamma(s)$, is a helix on $Out(\mathbf{w}, +)$ accumulating on the circle $Out(\mathbf{w}, +) \cap W_{loc}^u(\mathbf{w})$ because $x(s)$ and $y(s)$ are monotonic functions and:

$$\lim_{s \rightarrow 1^-} x(s) = +\infty \quad \text{and} \quad \lim_{s \rightarrow 1^-} y(s) = 0.$$

A similar proof may be constructed for a segment on $In(\mathbf{v}, -)$. Let n_0 be smallest value of $2n_0\pi$ such that both vertical boundaries of the rectangle $R_{\mathbf{w}}$ centered at $P_{\mathbf{w}} \leftrightarrow (0, 2\pi n_0)$ cuts the helix $\eta \circ \gamma(s)$ as shown in figure 6.

The sequences a_i and b_i defining the family of intervals are obtained from points where the helix $\eta(\gamma(s))$ meets the vertical boundaries of $R_{\mathbf{w}}$ defined locally by $\{\pm\varepsilon + 2n\pi\}_{n \geq n_0} \times [0, \tau]$. Solving the equation $x(s) = \pm\varepsilon + 2n\pi$ ($n \geq n_0$) with respect to y^* we get $y^* = e^{a_n}$ and $y^* = e^{b_n}$ where:

$$a_n = K^{-1}(-\varepsilon - 2n\pi + x_0) \quad \text{and} \quad b_n = K^{-1}(\varepsilon - 2n\pi + x_0).$$

□

The constant δ that appear in the proof is often called the *saddle value* of the cycle. Our choice of orientation around the heteroclinic connection $[\mathbf{v} \rightarrow \mathbf{w}]$, the hypothesis (H4), reflects what is observed numerically in the example described in Rodrigues and Labouriau [19]. If we had taken the rotation in W with the opposite orientation, then the two rotations in V and W would cancel out. While hypothesis (H1)–(H3) set up the structure of the Bykov cycle, hypothesis (H4) is needed because in the general case, the image of the spiral $\Psi_{\mathbf{v} \rightarrow \mathbf{w}} \circ \Phi_{\mathbf{v}} \circ \gamma(s)$ under $\Phi_{\mathbf{w}}$, may present reversals around $Out(\mathbf{w})$ and thus heteroclinic tangencies. This is beyond the scope of this article.

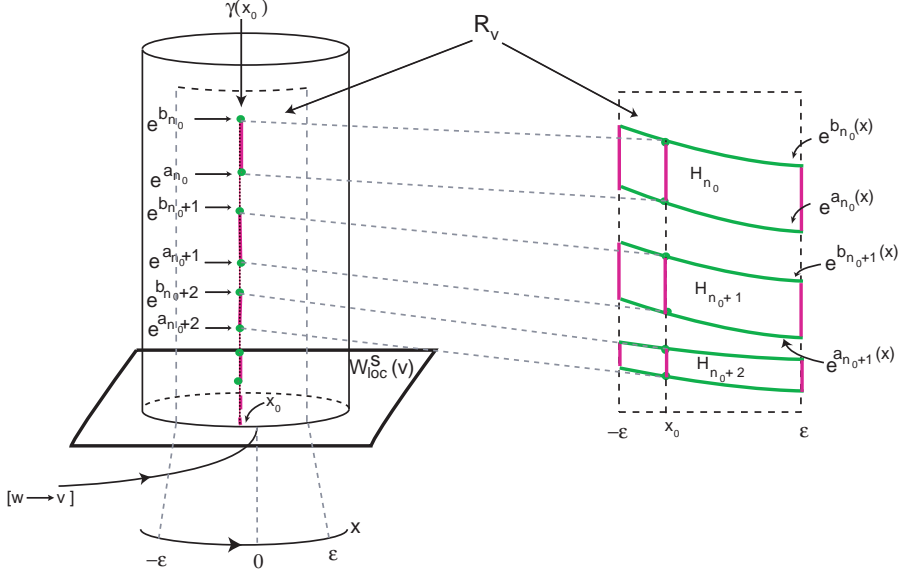


FIGURE 7. On a segment $\gamma \in In(\mathbf{v})$, there are infinitely many segments that are mapped by $\eta_{(1,1)}$ into $R_{\mathbf{w}}$. Varying $x \in [-\varepsilon, \varepsilon]$, each segment gives rise to a horizontal rectangle across $R_{\mathbf{v}} \subset In(\mathbf{v})$.

Observe that a_i and b_i are such that (see figure 7):

$$\forall i \geq n_0, \quad 1 > e^{b_i} > e^{a_i} > e^{b_{i+1}} \quad \text{and} \quad \lim_{i \geq n_0} e^{a_i} = \lim_{i \geq n_0} e^{b_i} = 0.$$

Our goal now is to use the *Generalized Conley-Moser Conditions* [16, 22, 34] applied to the two-dimensional map $R_{(1,1)}$ in order to ensure the existence of a “thin” invariant set topologically conjugated to a Bernoulli shift. These conditions are a combination of geometric and analytical properties. The geometrical part consists of generalizing the notion of horizontal and vertical rectangles of Guckenheimer and Holmes [12] by allowing the boundaries to be Lipschitz curves¹, rather than straight lines: (i) horizontal rectangles are mapped into vertical rectangles (strip condition); (ii) horizontal boundaries are mapped into horizontal boundaries and vertical boundaries are mapped into vertical boundaries (hyperbolicity condition).

We recall some terminology about horizontal and vertical strips used in Guckenheimer and Holmes [12] and in Rodrigues *et al* [27] adapted to our purposes. Given a rectangular region \mathcal{R} in $In(\mathbf{v})$ or in $Out(\mathbf{w})$ parametrized by a rectangle $R = [w_1, w_2] \times [z_1, z_2]$, a *horizontal strip* in \mathcal{R} will be parametrized by:

$$\mathcal{H} = \{(x, y) : x \in [w_1, w_2], y \in [u_1(x), u_2(x)]\},$$

where $u_1, u_2 : [w_1, w_2] \rightarrow [z_1, z_2]$ are Lipschitz functions such that $u_1(x) < u_2(x)$. The *horizontal boundaries* of the strip are the lines parametrized by the graphs of the u_i , the *vertical boundaries* are the lines $\{w_i\} \times [u_1(w_i), u_2(w_i)]$ and its *height* is:

$$h = \max_{x \in [w_1, w_2]} (u_2(x) - u_1(x)).$$

A *vertical strip* across \mathcal{R} , its *width* and a *vertical rectangle* have similar definitions, with the roles of x and y reversed. For $d > 0$, a d -horizontal rectangle is a horizontal strip with height d and a d -vertical rectangle is a vertical strip with width d .

Since a_n and b_n of proposition 5 depend smoothly on the angular coordinate x of the vertical segment γ , then the sequence of horizontal strips:

$$H_n = [-\varepsilon, \varepsilon] \times [a_n(x), b_n(x)] \subset R_{\mathbf{v}}, \quad n \geq n_0 \in \mathbf{N}, \quad x \in [-\varepsilon, \varepsilon]$$

¹In our case, they are smooth.

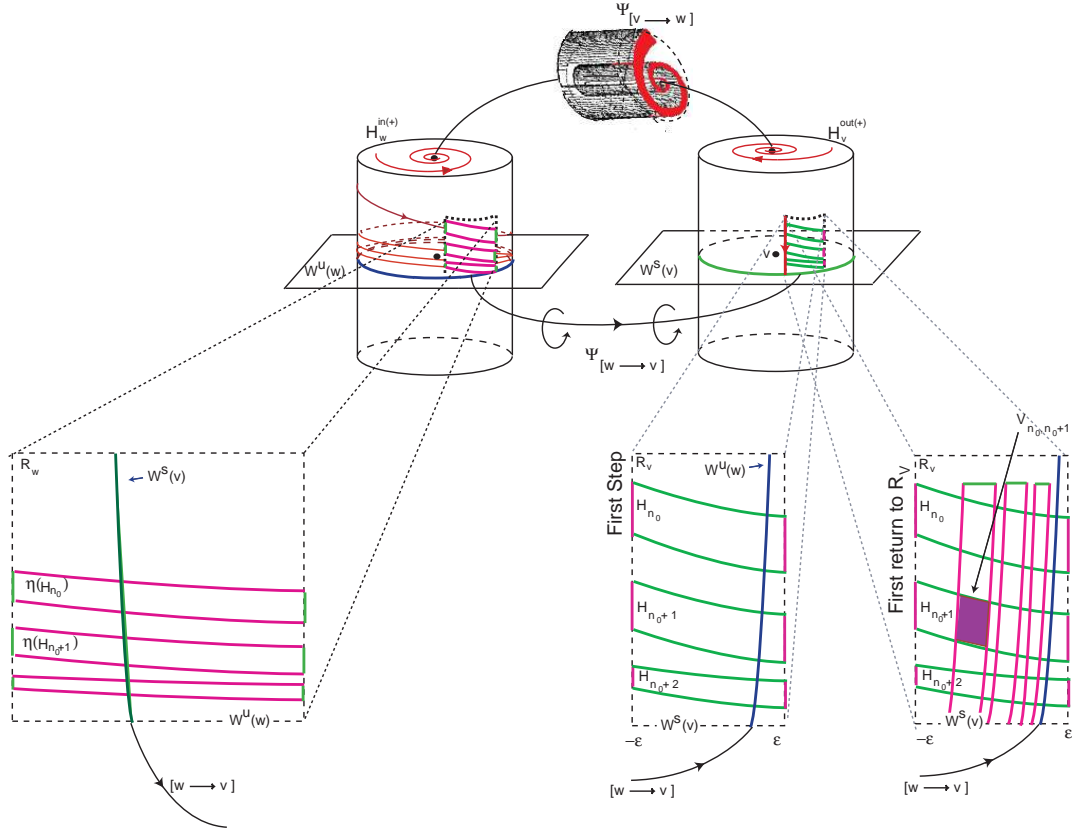


FIGURE 8. First return to $R_{\mathbf{v}}$: the image by η of a horizontal strip H_i across $R_{\mathbf{v}}$ is a horizontal strip across $R_{\mathbf{w}}$. The set $R(H_i)$ is a vertical strip across $R_{\mathbf{v}} \subset In(\mathbf{v})$.

are mapped by $\eta_{(1,1)}$ onto $R_{\mathbf{w}}$. The image under $\eta_{(1,1)}$ of the endpoints of the horizontal boundaries of H_n must join the end points of $\eta_{(1,1)}([e^{a_n}, e^{b_n}]) \subset R_{\mathbf{w}}$ – see figure 8. Moreover, if h_i denotes the height of the horizontal strip H_i then $\lim_{i \geq n_0} h_i = 0$.

Lemma 6. *For each $n > n_0$, the horizontal strip H_n is mapped by $R_{(1,1)}$ into a vertical strip across $R_{\mathbf{v}} \subset In(\mathbf{v})$.*

In the following proof, we omit the subscript $(1, 1)$.

Proof. For each $n > n_0$, denote by $\partial_v H_n$ the vertical boundaries of H_n . By proposition 5, the image by η of $\partial_v H_n$ is the graph of a smooth monotonically decreasing function in $Out(\mathbf{w})$ as shown in figure 6, being the horizontal boundary of the horizontal strip $\eta(H_n) \subset Out(\mathbf{w})$. Since $\Psi_{\mathbf{w} \rightarrow \mathbf{v}}$ can be seen as a rotation of $\frac{\pi}{2}$, the set

$$R(H_n) \cap R_{\mathbf{v}} =: V_n$$

is a vertical strip across $R_{\mathbf{v}} \subset In(\mathbf{v})$. □

Define $V_{ij} := R_{(1,1)}(H_i) \cap H_j$. By construction, for each $i, j \geq n_0$, the vertical boundaries of V_{ij} are contained in $R_{(1,1)}(H_i)$. Moreover, the image by $R_{(1,1)}$ of each horizontal boundary of H_i is a horizontal boundary of $R_{(1,1)}(H_i)$ as depicted in figures 8 and 9. Denoting by $\partial_v V_{ij}$ the vertical boundaries of V_{ij} , once again by construction, we have $R_{(1,1)}^{-1}(\partial_v V_{ij}) \subset \partial_v H_i$. Using proposition 5, lemma 6 and the above remark, we have demonstrated that:

Corollary 7 (Strip Condition). *There exist a infinite number of horizontal and vertical strips H_i and V_j ($i, j \geq n_0$) such that the map $R_{(1,1)}$ takes each H_i homeomorphically onto V_j , with horizontal boundaries mapped into horizontal boundaries and vertical boundaries mapped into vertical boundaries.*

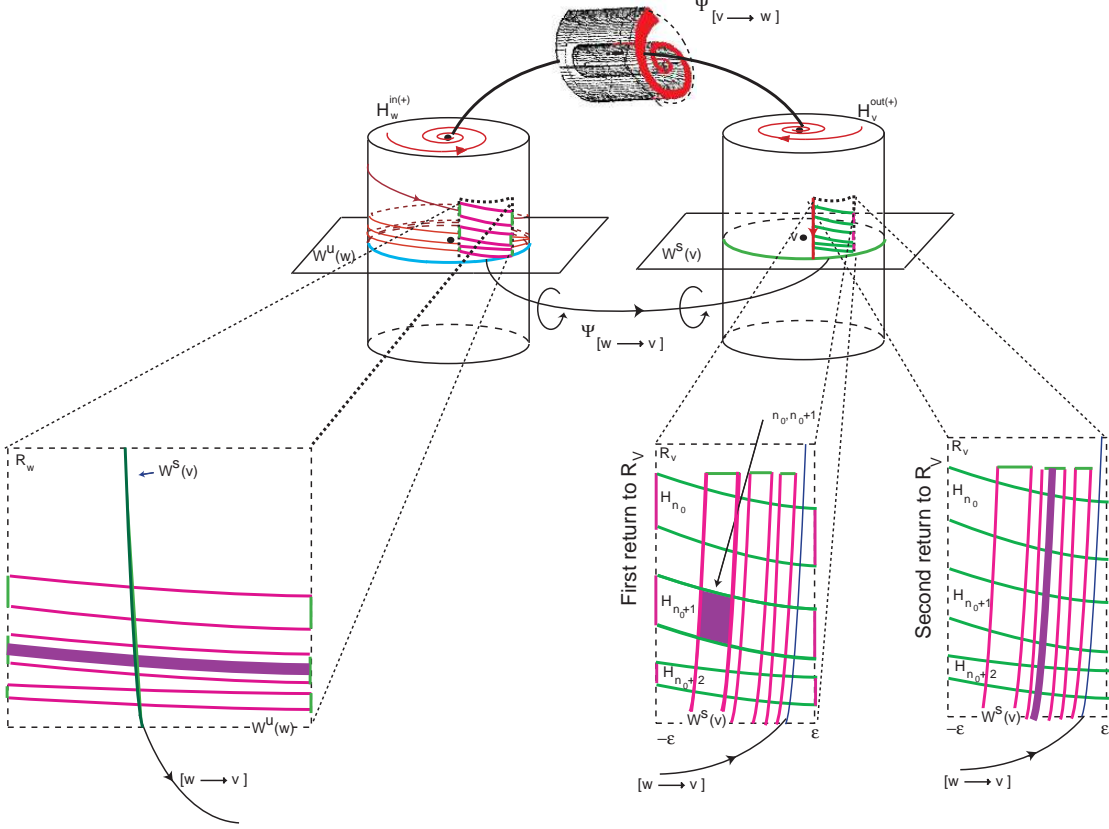


FIGURE 9. Second return to R_v : if $V_{ij} \subset H_i$ is a vertical strip across R_v , then $R(V_{ij}) \cap H_j \equiv \tilde{V}_j$ is a vertical strip across R_v .

Going backwards, we get dual results for a horizontal strip H_i across $In(\mathbf{v})$; indeed the set $\Psi_{\mathbf{w} \rightarrow \mathbf{v}}^{-1}(H_i)$ is a vertical strip across $R_{\mathbf{w}} \subset Out(\mathbf{w})$. The image of $\eta_{(1,1)}^{-1}$ of each vertical boundary of $\Psi_{\mathbf{w} \rightarrow \mathbf{v}}^{-1}(H_i)$ is a helix in $In(\mathbf{v})$ accumulating on $W^s(\mathbf{v})$, as illustrated in figure 10. It can be seen as the graph of a monotonically decreasing function in $In(\mathbf{v})$.

Lemma 8. *For each $i > n_0$, if H is a horizontal rectangle intersecting H_j fully, then $R_{(1,1)}^{-1}(H) \cap H_j \equiv \tilde{H}_i$ is a horizontal rectangle across R_v intersecting H_i fully.*

Define $H_{ij} := R_{(1,1)}^{-1}(H_j) \cap H_i$. Next lemma gives specific rates of contraction and expansion of H_i under $R_{(1,1)}$ along the horizontal and vertical directions. Note that these analytical conditions require uniform (but not constant) contraction in the horizontal direction and expansion in the vertical direction.

Lemma 9 (Hyperbolicity Condition). *There exist $\nu_h(n) < 1$ and $\nu_v(n) < 1$ such that:*

- (1) *if H is a d -horizontal strip which intersects H_i fully, then $R_{(1,1)}^{-1}(H) \cap H_i \equiv \tilde{H}_i$ is a D -horizontal strip with $D \leq \nu_h(n)d$ where $\nu_h(n) < 1$;*
- (2) *if V is a d -vertical strip contained in H_n , then $R_{(1,1)}(V) \cap H_j \equiv \tilde{V}_j$ is a D -vertical strip with $D < \nu_v(n)d$ where $\nu_v(n) < 1$;*

Proof. (1) If H is a d -horizontal strip which intersects H_i fully, then the rectangle $\Psi_{\mathbf{w} \rightarrow \mathbf{v}}^{-1}(H)$ is a vertical strip across $R_{\mathbf{w}}$. Its vertical boundaries are mapped by η^{-1} into a helix accumulating on $W_{loc}^s(\mathbf{v})$ – its graphs are smooth monotonically decreasing maps in $In(\mathbf{v})$, say y_1 and y_2 , both converging uniformly and exponentially to zero. Thus, the distance D is such that:

$$D \leq |y_2(x) - y_1(x)| \rightarrow 0,$$

and then the result follows (see figure 10). In this case, for n large enough, $\nu_h(n) \ll 1$.

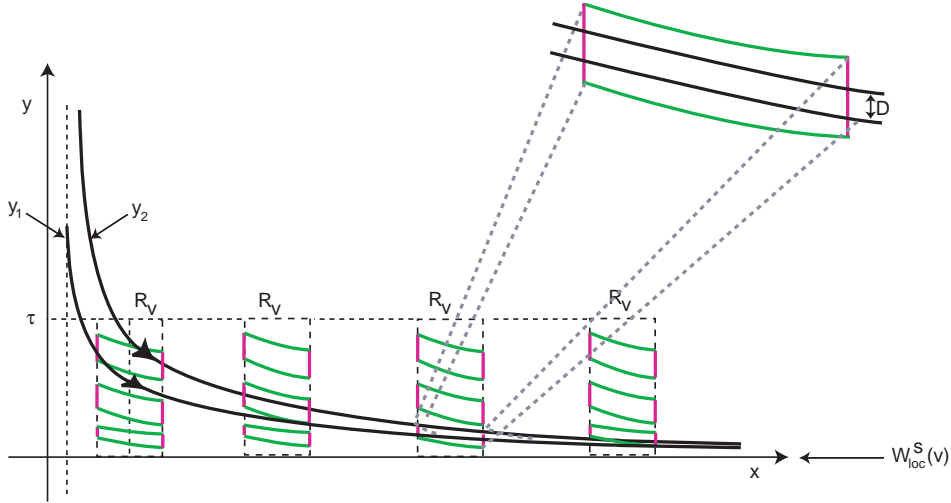


FIGURE 10. If H is a d -horizontal strip which intersects H_i fully, then the rectangle $\Psi_{\mathbf{w} \rightarrow \mathbf{v}}^{-1}(H)$ is a vertical strip across $R_{\mathbf{v}}$. Its vertical boundaries are mapped by η^{-1} into a helix accumulating on $W_{loc}^s(\mathbf{v})$.

- (2) If V_i is a d -vertical strip contained in H_j , then $\eta(V_i \cap H_j)$ is a horizontal strip across $Out(\mathbf{w})$, which is mapped by $\Psi_{\mathbf{w}, \mathbf{v}}$ into a vertical strip across $R_{\mathbf{v}} \subset In(\mathbf{v})$. The width D that we want to estimate is the height of $\eta(V_i \cap H_j) \cap R_{\mathbf{w}}$. The height D is the length of a segment connecting the image by η of two points of the type:

$$A \leftrightarrow (x_A, y_A) \quad \text{and} \quad B \leftrightarrow (x_B, y_B).$$

where $x_A, x_B \in [0, 2\pi]$, $x_B - x_A \approx d < 1$ and $y_B \approx y_A e^d$. The height of $\eta(V_i \cap H_j) \subset R_{\mathbf{w}}$ is given by

$$D \leq (y_A e^d)^\delta - y_A^\delta = y_A^\delta (e^{d\delta} - 1) = [d\delta + O(d^2)] y_A^\delta.$$

Since $x_0 \in [-\varepsilon, \varepsilon]$ with $\varepsilon > 0$ small, then for all $n \in \mathbf{N}$, we have $\varepsilon - 2n\pi + x_0 < 0$ and then

$$y_A^\delta = e^{K^{-1}\delta(\varepsilon - 2n\pi + x_0)} < 1$$

then it follows that $\nu_v(n) = y_A^\delta$. If $\delta > 1$, the result holds for n sufficiently large, say n_1 , meaning that perhaps we may need to shrink the cross section $R_{\mathbf{v}}$ to get the result (this is equivalent to neglect a finite number of horizontal rectangles R_n).

□

Remark 1. Recall that $\delta = \delta_{\mathbf{v}} \delta_{\mathbf{w}}$. The inequality $\delta > 1$ may be interpreted as: the product of the incoming velocities at the nodes is greater than the product of the outgoing velocities. This is particularly interesting for Bykov cycles that appear from the symmetry breaking networks as the one reported in [19].

The set trapped for two iterations forwards and two backwards is obtained by intersecting the thinner strips, yielding infinitely many smaller rectangles contained in those of the first stage as shown in figures 8 and 9. This process can be repeated *ad infinitum*. The spiralling non-wandering set associated to Γ is the intersection for all n , of the vertical and horizontal strips. It follows from the Generalized Conley-Moser conditions that:

Corollary 10. *There exists an invariant set of initial conditions $\Lambda \subset R_{\mathbf{v}} \subset In(\mathbf{v})$ on which the map $R_{(1,1)}|_{\Lambda}$ is topologically conjugate to a full shift over an infinite number of symbols.*

Saturating Λ with the flow, we obtain a set of zero Lebesgue three-dimensional measure. After infinitely many steps, what remains in $R_{\mathbf{v}}$ is a set of points Λ , which is in one-to-one correspondence with the set of bi-infinite sequences of a countable set of symbols. Some dynamical consequences of the conjugacy to a full shift over an infinite alphabet require careful analysis: the sequence $(H_n)_n$ converges to the lower boundary of $R_{\mathbf{v}}$ and $(\eta_{(1,1)}(H_n))_n$ converges to the lower boundary of $R_{\mathbf{w}}$, corresponding to the

the invariant manifolds of \mathbf{v} and \mathbf{w} , respectively. Note that in these cases, trajectories starting in $\partial R_{\mathbf{v}}$ and $\partial R_{\mathbf{w}}$ do not return to $R_{\mathbf{v}}$ and $R_{\mathbf{w}}$ under interaction by the first return map.

Taking \mathcal{V} as above and Σ as $R_{\mathbf{v}}$, we get the proof of theorem 1. Note that if $\delta \geq 1$, in order to apply the Generalized Conley-Moser conditions, we might neglect a finite number of horizontal rectangles in $R_{\mathbf{v}}$ to get the result, which is equivalent to shrink the cross section $R_{\mathbf{v}}$.

6. GENERAL GLOBAL MAPS

In the previous section, we assumed that the connection map $\Psi_{\mathbf{v} \rightarrow \mathbf{w}}$ was the identity map ($a = 1$). In this section, we discuss some modifications of the transition map and we show that our results continue to hold. Here, in rectangular coordinates, the diffeomorphism $\Psi_{\mathbf{v} \rightarrow \mathbf{w}}$ assumes the general form (6), that is:

$$\Psi_{\mathbf{v} \rightarrow \mathbf{w}}(X, Y) = \begin{pmatrix} a & 0 \\ 0 & \frac{1}{a} \end{pmatrix} \begin{pmatrix} X \\ Y \end{pmatrix}.$$

For $j \in \{+, -\}$, if $\gamma(s) = (x_0, y^*(s)) \in R_{\mathbf{v}} \subset \text{In}(\mathbf{v}, j)$ is a vertical segment on $\text{In}(\mathbf{v}, j)$, then the curve $\Phi_{\mathbf{v}} \circ \gamma(s)$ is still a spiral in $\text{Out}(\mathbf{v})$. Nevertheless the curve $(\Psi_{\mathbf{v} \rightarrow \mathbf{w}} \circ \Phi_{\mathbf{v}})(\gamma(s))$ is not a spiral because both components in $\text{In}(\mathbf{w})$ are not monotonic – see the wiggly curve in the rectangle of figure 11. The transformation (6) has the effect of enlarging the spiral $\Phi_{\mathbf{v}} \circ \gamma(s)$ by a factor of a in the horizontal direction and by a factor $\frac{1}{a}$ in the vertical direction. Therefore, the set $\eta_{(a, \frac{1}{a})}(\gamma(s))$ is a generalized helix.

Let S^a (resp. $S^{\frac{1}{a}}$) be the image by $\Psi_{\mathbf{v} \rightarrow \mathbf{w}}$ of the spiral $\Phi_{\mathbf{v}} \circ \gamma(s)$ obtained when the transition map from \mathbf{v} to \mathbf{w} is an uniform expansion of scalar factor $a > 1$ (resp. $a < 1$). In rectangular coordinates, this corresponds to $\Psi_{\mathbf{v} \rightarrow \mathbf{w}}(X, Y) = (aX, aY)$. Analogously, let H^a and $H^{\frac{1}{a}}$ be the corresponding helices. More precisely, we have

$$H^a = \Phi_{\mathbf{w}}(S^a) \quad \text{and} \quad H^{\frac{1}{a}} = \Phi_{\mathbf{w}}(S^{\frac{1}{a}}).$$

The next technical result will be useful in the sequel.

Lemma 11. *In rectangular coordinates, if $\Psi_{\mathbf{v} \rightarrow \mathbf{w}}$ is an uniform expansion (resp. contraction) of scalar factor a ($a > 0$), then:*

- (1) *the curve $\eta_{(a, a)}(\gamma(s))$ is a helix on $\text{Out}(\mathbf{w}, j)$ accumulating on the circle $\text{Out}(\mathbf{w}, j) \cap W^u(\mathbf{w})$.*
- (2) *there is $n_0 \in \mathbf{N}$ such that the points $y \in \text{In}(\mathbf{v})$ such that $\eta_{(a, a)}(y) \in \partial R_{\mathbf{w}}$ are given by $y = e^{a_n} a^{-1}$ and $y = e^{b_n} a^{-1}$, where $n \geq n_0$ and a_n, b_n are those defined in proposition 5.*

Proof. The proof of the above lemma is similar to that of proposition 5, taking into account this variation:

$$(\eta_{(a, a)} \circ \gamma)(s) = [-K \ln(ay^*(s)) + x_0; (ay^*(s))^\delta] = (x(s), y(s)).$$

- (1) Since $a > 0$, the curve $(\eta_{(a, a)} \circ \gamma)(s)$ is a helix on $\text{Out}(\mathbf{w}, +)$ accumulating on the circle $\text{Out}(\mathbf{w}, +) \cap W_{loc}^u(\mathbf{w})$ because $x(s)$ and $y(s)$ are monotonic maps and:

$$\lim_{s \rightarrow 1^-} x(s) = +\infty \quad \text{and} \quad \lim_{s \rightarrow 1^-} y(s) = 0.$$

- (2) Solving the equation $-k \ln(ay^*(s)) + x_0 = \pm \varepsilon + 2n\pi$ with respect to $y^*(s)$, we get

$$\ln(y^*(s)) = K^{-1}(\mp \varepsilon - 2n\pi + x_0) - \ln(a)$$

and then $y^*(s) = e^{a_n} a^{-1}$ and $y^*(s) = e^{b_n} a^{-1}$, where $n \geq n_0$. The sequences a_n, b_n are exactly the same as those sequences defined in proposition 5 – note that n_0 may not be the same. \square

For each $x \in [-\varepsilon, \varepsilon]$, the sequences a_n and b_n depend smoothly on the constant $a > 0$. Let $n_1 > n_0$ be the smallest value of $2n\pi$ such that both helices H^a and $H^{\frac{1}{a}}$ meet the rectangle $R_{\mathbf{w}}$ in both sides. Now, define the new rectangle

$$\mathcal{R}_{n_1} = [2\pi n_1, 2\pi(n_1 + 1)] \times [0, \tau],$$

which can be seen a cover of $\text{Out}(\mathbf{w})$. Restricted to \mathcal{R}_{n_1} , the graph of $(\eta_{(a, \frac{1}{a})} \circ \gamma)(s)$ is a generalized helix on $\text{Out}(\mathbf{w})$ turning once around the cylinder, as depicted in figure 11. For each $n > n_1$ and for each $x_0 \in [-\varepsilon, \varepsilon]$, there exists $\sigma_n(a, x_0), \rho_n(a, x_0)$ such that:

$$(\eta_{(a, a)} \circ \gamma)(\sigma_n(a, x_0)) \in \delta_l \mathcal{R}_{n_1} \quad \text{and} \quad (\eta_{(a, a)} \circ \gamma)(\rho_n(a, x_0)) \in \delta_r \mathcal{R}_{n_1},$$

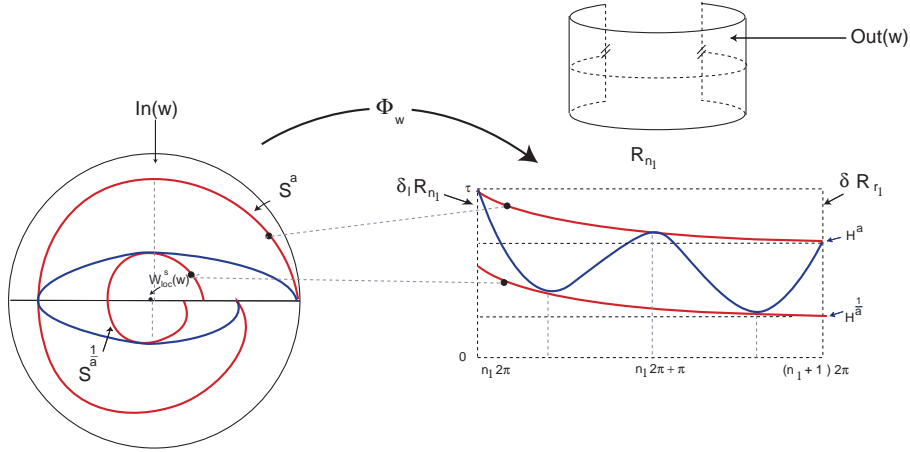


FIGURE 11. The transition map from \mathbf{v} to \mathbf{w} may be approximated by a diagonal map. S^a (resp. $S^{\frac{1}{a}}$) corresponds to the spiral $\Psi_{\mathbf{v} \rightarrow \mathbf{w}} \circ \Phi_{\mathbf{v}} \circ \gamma(s)$, where $\Psi_{\mathbf{v} \rightarrow \mathbf{w}}$ is a uniform expansion of ratio a (resp. contraction of ratio $\frac{1}{a}$). The image of S^a by $\Phi_{\mathbf{w}}$ is the upper helix H^a and that of $S^{\frac{1}{a}}$ is the lower helix $H^{\frac{1}{a}}$. The generalized spiral in blue is mapped under $\Phi_{\mathbf{w}}$ into a generalized helix on $Out(\mathbf{w})$ accumulating on the unstable manifold of \mathbf{w} (x -axis).

where $\partial_l \mathcal{R}_{n_1}$ and $\partial_r \mathcal{R}_{n_1}$ represent the left and the right vertical boundaries of \mathcal{R}_{n_1} . Explicitly, these sequences depend on a and they are given by:

$$\sigma_n(a, x_0) = a^{-1} e^{K^{-1}(-2n\pi + x_0)} \quad \text{and} \quad \rho_n(a, x_0) = a^{-1} e^{K^{-1}(-2(n+1)\pi + x_0)},$$

which converge exponentially fast to zero. Depending of the angle of $\varphi \in [0, 2\pi[\pmod{2\pi}$ in $In(\mathbf{w})$, the spiral S^a has different expansion and contraction. Thus for each $\tilde{a} \in [\frac{1}{a}, a]$, we define the curve of points in the plane $x = x_0$ that are the pre-image of the generalized helix $(\eta_{(\tilde{a}, \frac{1}{\tilde{a}})} \circ \gamma)(s)$ as plotted in figure 12. The pre-image of the vertical boundaries of $R_{\mathbf{w}}$ by $\eta_{(\tilde{a}, \frac{1}{\tilde{a}})}$ intersect twice this graph, say $l_n(x_0)$ and $u_n(x_0)$. Hence, we may define the maps $l_n(x)$ and $u_n(x)$, which depend smoothly on x . It is easy to see that:

$$[l_n(x), u_n(x)] \subset [\sigma_n(a, x), \rho_n(a, x)],$$

whose length tends to zero. For each $n > n_1$, defining the horizontal rectangle:

$$\mathcal{H}_n = \{(x, y) \in In(\mathbf{v}) : x \in [-\varepsilon, \varepsilon] \text{ and } y \in [l_n(x), u_n(x)]\},$$

theorem 1 and its proof go through in the same manner. The geometry of the horseshoe may be more complicated.

7. DISCUSSION AND FINAL REMARKS

7.1. Generalization. Not all conditions (H1) are essential to prove that Bykov cycles are repelling: the eigenvalues of df at \mathbf{v} and \mathbf{w} may have any imaginary part not necessarily 1. The rotation around each saddle-focus is very different from the situation where all eigenvalues are real, nevertheless our proof also runs if the eigenvalues of df of one node had only real eigenvalues. The proof is still valid for any finite number of one-dimensional heteroclinic connections from \mathbf{w} to \mathbf{v} . Theorem 1 can be easily generalized to heteroclinic network of rotating nodes as defined in Aguiar *et al* [2], involving any finite number of rotation nodes. Of course, our result holds for any measure equivalent to the Lebesgue two-dimensional measure on the cross section – note that *equivalent* means the same null sets.

Bowen constructed a horseshoe for a diffeomorphism of a two-dimensional disk in the standard way, with the difference that he allows the Cantor set to be “fat” – at each step in the construction, the author deletes a decreasing proportion of the remaining sets. Controlling this rate, he obtained a hyperbolic Cantor set of positive one-dimensional measure. The product of this set with itself gives rise to a Cantor set with two-dimensional Lebesgue measure, which is a Milnor attractor. In our article, we proved that the chain of horseshoes semiconjugate to full shifts over an alphabet with more and more symbols, is not of the same kind to that of [6] because it occupies a zero Lebesgue measure.

7.4. Examples. Explicit examples of vector fields for which such a Bykov cycle can be found analytically are reported in Aguiar *et al* [1] and Rodrigues and Labouriau [19] – there, the authors first constructed an explicit $(\mathbf{SO}(2) \oplus \mathbf{Z}_2)$ -equivariant differential equation whose flow has an globally attracting three-dimensional sphere, containing an attracting heteroclinic network involving two saddle-foci of different Morse indices (*ie*, (H1) and (H2) are verified). By adding non-equivariant terms, the $\mathbf{SO}(2)$ -symmetry is broken and so are the two dimensional heteroclinic connections. The symmetry-breaking terms are tangent to the invariant sphere so it is still invariant. The equilibria are preserved together with their stability. Using Melnikov method, the authors proved that the two-dimensional invariant manifolds intersect transversely (*ie*, (H3) holds). Hypothesis (H4) is valid because of the method *lifting by rotation* used to construct vector fields described in [1] and [27]. Because of the reinjection mechanisms built into these networks, trajectories will make repeated passes near the transversal intersections and there are trajectories that follow arbitrarily complicated paths around the network.

7.5. Numerics. Finally, we would like to stress that in some packages of numerical simulations, a trajectory tending to a robust heteroclinic cycle will continue to approach until the numerical error is greater than the distance between the solution and the invariant space. Usually, the program assumes that the solution has been captured by a periodic solution. This is why in some cases typical trajectories near Bykov cycles seem to be near the cycle for all time, which is not the real case – numerical simulations have been presented in Aguiar *et al* [1] and Rodrigues and Labouriau [19]. Hence, the present paper should alert those that doing numerical simulations near heteroclinic structures deduce that the network is stable because trajectories are observed to approach it.

Acknowledgements: The author would like to express his gratitude to Isabel Labouriau and Mário Bessa for helpful discussions.

REFERENCES

- [1] M. Aguiar, S. B. Castro, I. S. Labouriau, *Simple Vector Fields with Complex Behaviour*, Int. Jour. of Bifurcation and Chaos, Vol. 16, No. 2, 369–381, 2006
- [2] M.A.D. Aguiar, I. S. Labouriau, A.A.P. Rodrigues, *Switching near a heteroclinic network of rotating nodes*, Dynamical Systems: an International Journal, Vol. 25, Issue 1, 75–95, 2010
- [3] W. Brannath, *Heteroclinic networks on the tetrahedron*, Nonlinearity 7, 1367–1384, 1994
- [4] G. D. Birkhoff, *Dynamical Systems*, Amer. Math. Soc., Colloquium Publications, 9, 1927
- [5] G. D. Birkhoff, *Nouvelles Recherches sur les systèmes dynamiques*, Memorie Pont Acad Sci. Novo. Lyncaei, Vol. 53, 1, 85–216, 1935
- [6] R. Bowen, *A horseshoe with positive measure*, Invent. Math. 29, 203–204, 1975
- [7] R. Bowen, *Equilibrium States and the Ergodic Theory of Anosov Diffeomorphisms*, Lect. Notes in Math, Springer, 1975
- [8] J. Buescu, *Exotic Attractors*, Progress in mathematics, Vol. 153, Birkhauser Verlag, 1997
- [9] V. V. Bykov, *Orbit Structure in a Neighbourhood of a Separatrix Cycle Containing Two Saddle-Foci*, Amer. Math. Soc. Transl, Vol. 200, 87–97, 2000
- [10] F. Fernández-Sánchez, E. Freire, A. J. Rodríguez-Luis, *T-Points in a \mathbf{Z}_2 -Symmetric Electronic Oscillator. (I) Analysis*, Nonlinear Dynamics, 28, 53–69, 2002
- [11] M. Field, *Lectures on bifurcations, dynamics and symmetry*, Pitman Research Notes in Mathematics Series, Vol. 356, Longman, 1996
- [12] J. Guckenheimer, P. Holmes, *Nonlinear Oscillations, Dynamical Systems, and Bifurcations of Vector Fields*, Applied Mathematical Sciences, 42, Springer-Verlag, 1983
- [13] A. J. Homburg, *Periodic attractors, strange attractors and hyperbolic dynamics near homoclinic orbit to a saddle-focus equilibria*, Nonlinearity 15, 411–428, 2002
- [14] A. J. Homburg, B. Sandstede, *Homoclinic and Heteroclinic Bifurcations in Vector Fields*, Handbook of Dynamical Systems, Vol. 3, North Holland, Amsterdam, 379–524, 2010

- [15] S. Ibáñez, J. A. Rodríguez, *Shilnikov configurations in any generic unfolding of the nilpotent singularity of codimension three in \mathbf{R}^3* , Journal of Differential Equations, 208, 147–175, 2008
- [16] W.S. Koon, M. Lo, J. Marsden, S. Ross, *Heteroclinic connections between periodic orbits and resonance transition in celestial mechanics*, Control and Dynamical Systems Seminar, California Institute of Technology, Pasadena, California, 1999
- [17] M. Krupa, I. Melbourne, *Asymptotic Stability of Heteroclinic Cycles in Systems with Symmetry*, Ergodic Theory and Dynam. Sys., Vol. 15, 121–147, 1995
- [18] M. Krupa, I. Melbourne, *Asymptotic Stability of Heteroclinic Cycles in Systems with Symmetry, II*, Proc. Roy. Soc. Edinburgh, 134A, 1177–1197, 2004
- [19] I. S. Labouriau, A. A. P. Rodrigues, *Spiraling sets near a heteroclinic network*, submitted
- [20] J. Milnor. *On the concept of attractor*, Commun. Math. Phys., 99, 177–195, 1985
- [21] L. Mora, M. Viana, *Abundance of strange attractors*, Acta Math. 171, 1–71, 1993
- [22] J. Moser, *Stable and Random Motions in Dynamical Systems*, Princeton University Press, Princeton, 1973
- [23] O. Podvigina, P. Ashwin, *On local attraction properties and a stability index for heteroclinic connections*, Nonlinearity 24, 887–929, 2011
- [24] H. Poincaré, *Sur le problème des trois corps et les équations de la dynamique*, Acta Mathematica, 13, 1–270, 1890
- [25] A. A. P. Rodrigues, *Persistent Switching near a Heteroclinic Model for the Geodynamo Problem*, Chaos, Solitons & Fractals, to appear, 2013
- [26] A. A. P. Rodrigues, I. S. Labouriau, *Global generic dynamics close to symmetry*, Journal of Differential Equations, Journal of Differential Equations, Vol. 253 (8), 2527–2557, 2012
- [27] A. A. P. Rodrigues, I. S. Labouriau, M. A. D. Aguiar, *Chaotic Double Cycling*, Dynamical Systems: an International Journal, Vol. 26, Issue 2, 199–233, 2011
- [28] V. S. Samovol, *Linearization of a system of differential equations in the neighbourhood of a singular point*, Sov. Math. Dokl, Vol. 13, 1255–1959, 1972
- [29] L. P. Shilnikov, *Some cases of generation of periodic motion from singular trajectories*, Math. USSR Sbornik (61), 103. 443–466, 1963
- [30] L. P. Shilnikov, *A case of the existence of a denumerable set of periodic motions*, Sov. Math. Dokl, No. 6, 163–166, 1965
- [31] L. P. Shilnikov, *The existence of a denumerable set of periodic motions in four dimensional space in an extended neighbourhood of a saddle-focus*, Sovit Math. Dokl., 8(1), 54–58, 1967
- [32] S. Smale, *Diffeomorphisms with many periodic orbits*, Diff. Comb. Topology, ed. S. Cairus, Princeton University Press, 63–86, 1960
- [33] S. Smale, *Differentiable dynamical systems*, Bull. Amer. Math. Soc., 73, 747–817, 1967
- [34] S. Wiggins, *Introduction in Applied Nonlinear Dynamical Systems and Chaos*, Springer-Verlag, TAM 2, New York, 1990

(A. A. P. Rodrigues) CENTRO DE MATEMÁTICA DA UNIVERSIDADE DO PORTO, AND FACULDADE DE CIÊNCIAS DA UNIVERSIDADE DO PORTO, RUA DO CAMPO ALEGRE 687, 4169–007 PORTO, PORTUGAL
E-mail address, A.A.P.Rodrigues: alexandre.rodrigues@fc.up.pt